Unoccupied States in C_{60} Thin Films Probed by Two-Photon Photoemission

Gregory Dutton and X.-Y. Zhu*

Department of Chemistry, University of Minnesota, Minneapolis, Minnesota 55455

Received: February 18, 2002; In Final Form: April 29, 2002

Unoccupied electronic states in C_{60} thin films on Cu(111) have been measured by laser two-photon photoemission (2PPE) spectroscopy. These measurements allow the quantitative determination of energetic positions for the lowest unoccupied molecular orbital (LUMO), LUMO + 1, LUMO + 2, image potential states, as well as the highest occupied molecular orbital (HOMO). The transiently populated LUMO and LUMO + 1 levels are stabilized by the on-molecule charge correlation energy during the 2PPE process. Compared to previous measurements using one-photon photoemission and inverse photoemission, the HOMO−LUMO gap determined by 2PPE is stabilized by half of the Hubbard U. Both intramolecular excitation and a minor metal-to-molecule electron-transfer excitation channel are observed.

1. Introduction

Molecular seminconductors have attracted research interests from a number of fields, ranging from chemistry and physics to materials science and electrical engineering. These interests have surged recently following successes in a wide variety of electronic and optoelectronic devices from molecular materials, particularly the spectacular demonstration of high-mobility field-effect transistors (FETs) and superconducting FETs in molecular crystals.[2] A key issue in designing and developing electronic and optoelectronic devices from molecular solids is to understand the electronic structure, i.e., occupied and unoccupied orbitals or bands. Past attempts in characterizing electronic structure of molecular solids have relied predominantly on ultraviolet photoemission spectroscopy (PES) for occupied states and inverse photoemission spectroscopy (IPES) for unoccupied states. Recently, laser two-photon photoemission (2PPE) spectroscopy has emerged as a successful alternative.[3] It is capable of determining both occupied and unoccupied states. A particular advantage of this technique over PES and IPES is that 2PPE can be carried out in a time-resolved fashion for the determination of electron dynamics on a femtosecond time scale.[4,5] As part of a systematic effort to develop 2PPE as a viable technique for determining the electronic structure and electron dynamics in molecular semiconductors and at molecular semiconductor/metal interfaces,[6] we apply 2PPE to a model system: thin films of C_{60} adsorbed on Cu(111). The C_{60} system is chosen because it is the best understood and most extensively studied molecular semiconductor. The wealth of information on the electronic structure of C_{60} from extensive experiment[7,8] and theory[9,10] allows a reliable and quantitative interpretation of 2PPE results.

The optical band gap of C_{60} in the condensed phase is $\Delta = 2-2.2$ eV.[6,7] This gap corresponds to the dipole forbidden excitation of one electron from the highest occupied molecular orbital (HOMO) to the lowest unoccupied molecular orbital (LUMO), which gives an *N*-electron, neutral, singlet state. Here, *N* represents the total number of electrons in the system. On the other hand, the HOMO−LUMO gap determined by PES and IPES is 3.5−3.7 eV.[6,7] PES and IPES give ionization potential (IP, $N - 1$ electron final state) and electron affinity (EA, $N + 1$ electron final state), respectively. The difference between (IP−EA) and Δ is the so-called Hubbard U ($= 1.6 \pm 0.2$ eV), i.e., the on-molecule, charge−charge interaction energy.[6,7,11] Because the Hubbard U is larger than the bandwidth (≤ 0.5 eV), C_{60} is a strongly correlated Mott−Hubbard-type solid.

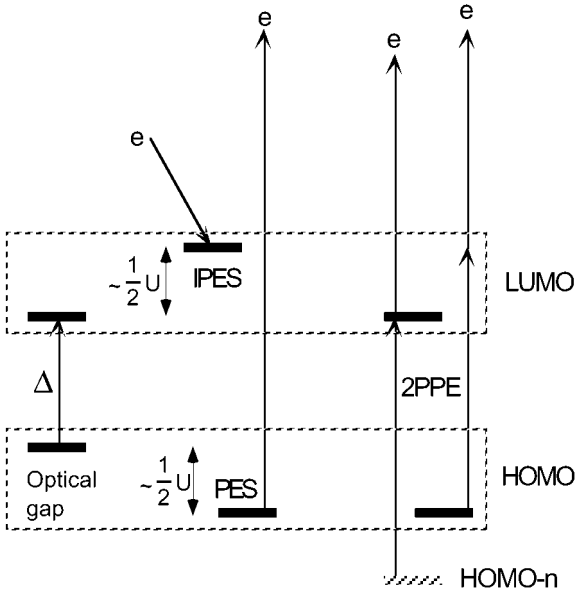

Figure 1. Energy level diagram showing the optical band gap (Δ) on the left, the transport band gap determined by PES and IPES in the middle, and the HOMO−LUMO gap determined by 2PPE on the right.

Two-photon photoemission (2PPE) spectroscopy probes both occupied and unoccupied states. It is compared to optical absorption, PES, and IPES in Figure 1. As far as HOMO is concerned, the 2PPE process gives an $N - 1$ electron final state, yielding the IP, same as in PES. However, when LUMO is involved in such a strongly correlated solid, the 2PPE process may not give the EA. The first step in 2PPE may involve intramolecular excitation, which promotes one electron from an occupied orbital, HOMO $- n$ ($n \geq 0$), to the LUMO. Absorption of the second photon ionizes the LUMO level. This transiently populated LUMO level is stabilized by the exciton-like electron−hole attraction. Because only the LUMO is

* Corresponding author. E-mail: zhu@chem.umn.edu.

10.1021/jp0256589 CCC: $22.00
Published on Web 06/06/2002

stabilized, not the HOMO, we believe the band gap of solid C_{60} determined by 2PPE is given by $\Delta + 1/2U$. On the other hand, the LUMO may also be populated by intermolecular charge-transfer excitation (or substrate-to-molecule charge transfer when C_{60} is adsorbed on a surface). In this case, the LUMO position determined by 2PPE may approach that from IPES.

The model system of C_{60} on the Cu(111) surface has been studied extensively before.[12−14] Monolayer C_{60} interacts strongly with Cu(111) and forms a (4×4) superlattice, with a lattice parameter only 1.7% larger than that in solid C_{60}. Subsequent deposition of C_{60} leads to the epitaxial growth of thin films. There is charge transfer of 1−2 electrons per molecule from the Cu(111) surface to the C_{60} monolayer.[11−14] As a result, the electronic structure of the first layer is distinctly different from molecules in multilayers. Interestingly, photoemission studies of C_{60} on Cu(111)[11−13,15] and other metal surfaces,[16−21] showed that the work function of C_{60} monolayer covered metal is ∼5 eV, independent of the metal involved. This has been interpreted as the work function of a metallic-like C_{60} surface, a result of substrate-to-C_{60} electron transfer.

There have been several two-photon photoemission studies of C_{60} thin films. Quast et al. studied a chemisorbed monolayer of C_{60} on Ni(110) by a combination of picosecond lasers and synchrotron radiation.[22] These authors attributed a transiently populated feature at ∼1.8 eV above E_{Fermi} to the LUMO + 1 level, formed by photoexcitation from filled states near or below the Fermi level. Long et al. measured photoelectron spectra from singlet and triplet excitons and reported a 0.33 eV difference between the two states.[23] Jacquemin et al. reported a time-resolved 2PPE measurement with limited energy resolution of thin C_{60} films condensed on polycrystalline Cu.[24]

2. Experimental Section

All experiments were performed in an ultrahigh vacuum (UHV) chamber with a base pressure of 7×10^{-11} Torr. The substrate was a single-crystal copper disk cut and polished to within 1° of the (111) plane. The sample could be liquid nitrogen cooled to 100 K and resistively heated. Cleaning was achieved by cycles of 1 keV Ar^+ sputtering at 10 μA followed by annealing at 760 K. Substrate cleanliness was routinely monitored by Auger electron spectroscopy (AES), low energy electron diffraction (LEED), and 2PPE. Cleaning cycles were repeated until AES showed surface carbon coverage less than 2%, LEED gave a sharp (1×1) pattern, and 2PPE yielded sharp Cu(111) surface state and image state features.

Fullerene, C_{60} (99.9+%, Alfa Aesar), well degassed in a vacuum at elevated temperature, was dosed onto the clean substrate by thermal evaporation at 400 °C from a tantalum foil cylinder with an exit aperture 50 mm from the surface. The doser could be rapidly heated by backside electron bombardment from a hot tungsten filament. During the brief temperature ramp-up period, the sample surface was rotated to face away from the dosing aperture and translated out of line-of-sight, and the increase in chamber pressure was less than 1 order of magnitude. Reproducible exposures were obtained by accurate control of dosing temperature. Once prepared, the persistent C_{60} monolayer resists removal by sputtering. We find that an initial higher ion energy sputtering cycle at 1.5 keV Ar^+ is necessary to recover the clean surface for preparation of subsequent films. All measurents were performed on films freshly prepared on a clean substrate.

The experimental apparatus used is depicted in Figure 2. Laser light for photoemission was generated by a Ti:sapphire oscillator

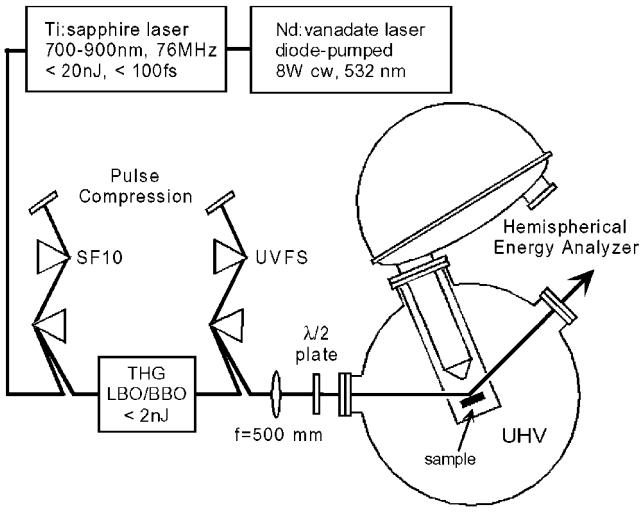

Figure 2. Experimental setup.

(Coherent MIRA 900) pumped by an 8 W cw solid-state pump (Coherent Verdi-V8) at 532 nm. The tunable wavelength Ti:sapphire fundamental (76 MHz, 0.8−1.5 W, 700−900 nm, < 70 fs) was frequency tripled in an ultrafast harmonic generator package (INRAD 5−050) to obtain photon energies from 4 to 5 eV. Prism pairs for dispersion compensation both before and after harmonic generation allowed minimization of pulse width for maximum harmonic conversion and 2PPE signal. Autocorrelation measurement using two-photon photoemission features from occupied states gave a pulse width of 50 fs in the UV region. In the experiments presented here, the two photons required for photoemission were derived from the same pulse.

Photoelectrons were detected with a hemispherical electron energy analyzer (Vacuum Generators 100AX) with an instrumental resolution of 35 meV, determined by fitting the Fermi edge of the cooled copper sample with an instrumentally broadened Fermi-Dirac distribution. This experimental broadening is dominated by the bandwidth of the laser pulses. The width of the narrowest feature observed, the clean Cu(111) $n = 1$ image state, was < 80 meV fwhm. All spectra were recorded at a pass energy of 1 eV. The spectrometer was encased in a μ-metal shield with small holes for sample and laser access to minimize deflection of the low energy photoelectrons by the Earth and stray magnetic fields. The sample was oriented normal to the spectrometer for all measurements. The UV pulses, p-polarized and incident at 60° from the spectrometer axis, were brought to a 60−70 μm focus at the sample surface. A bias of −1 V was applied to the sample during measurement to allow clear observation of the low energy vacuum edge for determination of work function. Comparison with spectra taken from a grounded sample showed no change in peak position or dispersion due to this slight bias voltage. Typical laser pulse fluence was 15 mJ/cm^2, and no evidence of space charge effects was observed at this fluence level.

3. Results

3.1. C_{60} Adsorption and Coverage Calibration. Before presenting 2PPE results, we first address the adsorption of C_{60} on Cu(111) and surface coverage calibration. Calibration of C_{60} coverage was achieved by monitoring the attenuation of the 920 eV copper Auger line and the growth of the 272 eV carbon line as a function of exposure. C_{60} is known to interact more strongly with noble metal surfaces than the weak van der Waals cohesion of the molecules in the bulk.[11−20] Multilayers desorb at temperatures <250 °C, while the monolayer persists on

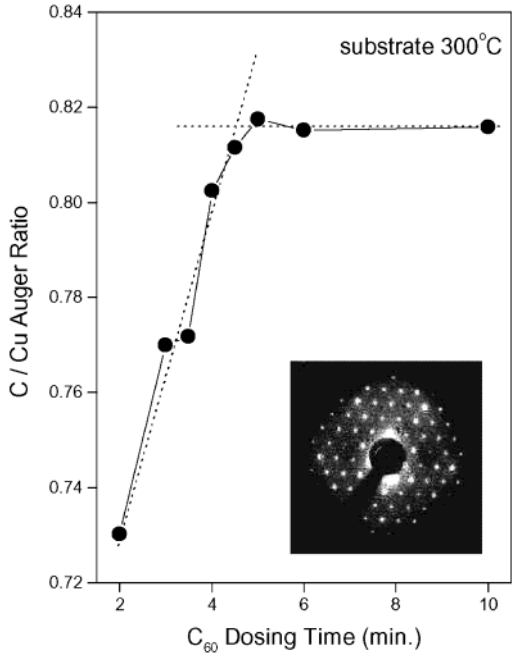

Figure 3. C (272 eV) to Cu (920 eV) Auger peak ratio as a function of dosing time for C_{60} on Cu(11) at a substrate temperature of 300 °C. The interception of the two dashed lines represents the point of monolayer formation. The inset shows a (4 × 4) LEED pattern of the monolayer-covered surface.

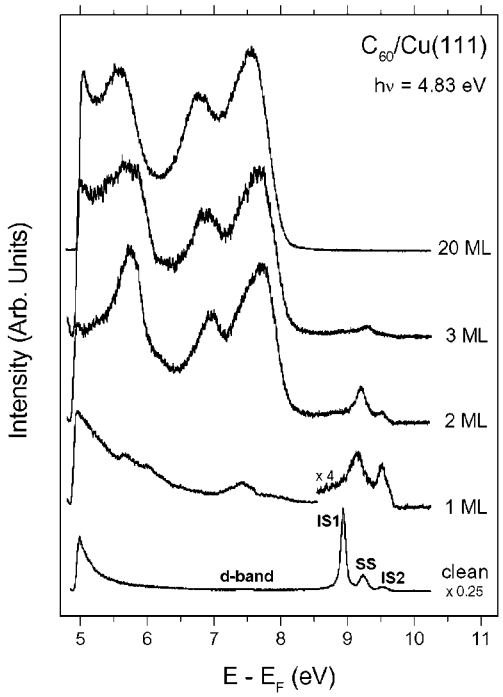

Figure 4. 2PPE spectra taken at a photon energy of 4.83 eV for clean and C_{60} covered Cu(111) surfaces at various coverages (1−20 ML). SS: surface state; IS1 and IS2: image states ($n = 1, 2$).

Cu(111) to at least 500 °C and is believed to decompose at higher temperatures rather than desorb molecularly.[11−13] This allows for facile and reliable preparation of monolayers by dosing in excess on a substrate held at 300 °C.

A calibration curve for saturation of 1 monolayer (ML) C_{60} as monitored by AES is presented in Figure 3. A slow deposition rate of 0.22 ML/min was obtained. Alternatively, it is possible to dose onto the substrate at room temperature and subsequently anneal off multilayers, an approach which has commonly been applied in previous work. We have found that elevated substrate temperature during dosing is critical for the growth of highly crystalline epitaxial films. The LEED image of a monolayer deposited at 300 °C (inset, Figure 3) displayed a sharp (4 × 4) pattern, while that of a room temperature deposited monolayer yielded diffuse spots. Additionally, 2PPE spectra of image states, which are sensitive to film morphology and crystallinity, provide further evidence that elevated substrate temperature during dosing yields high quality monolayer and multilayer films. Image state results will be further discussed below. The preferred recipe employed in the present work for preparing multilayers was to first deposit a monolayer at 300 °C, cool the substrate to 150 °C (safely below the multilayer desorption temperature), and meter further exposure time. All coverages were calibrated against the monolayer coverage in Figure 3 based on Auger ratios. A constant sticking coefficient is assumed for all coverages at the substrate dosing temperature of 150 °C.

3.2. 2PPE Spectra. Two-photon photoemission spectra recorded at a photon energy of 4.83 eV from various coverages of C_{60} on Cu(111) are presented in Figure 4. The spectra are plotted as total final photoelectron energy referenced to the copper Fermi level. Thus the position of the low energy vacuum cutoff represents the value of the work function, Φ, for each surface. For the clean surface we obtain a value of $\Phi = 4.94$ eV, which decreases to 4.89 eV at 1 ML and recovers to 4.95 eV for thicker films, in general agreement with previous photoemission studies.[11−13] A photon energy of 4.83 eV therefore renders accessible all unoccupied states to within ∼100 meV of the vacuum level. The clean Cu(111) spectrum is dominated by the unoccupied $n = 1$ and $n = 2$ image states (IS1, IS2) and the well-known occupied Shockley surface state (SS).[2] Discernible at smaller scales is a feature at ∼7.5 eV arising from the copper d-band, as well as emission from the broad copper sp-band apparent as a weak structureless background extending to the Fermi edge. With the adsorption of 1 ML C_{60}, the surface state is completely quenched while the image states remain. With the exception of these relatively sharp image states, the effect of the monolayer on the spectrum is limited to a few weak features superimposed on the copper substrate spectrum. Further increasing the coverage to 2 ML leads to a dramatic change in the 2PPE spectrum. Several broad, intense peaks appear to dominate at all coverages investigated. These features remain nearly unchanged when the C_{60} coverage is increased from 2 to 20 ML, which presumably approaches the characteristics of bulk C_{60}.

The origins of photoelectrons from occupied and unoccupied states can be easily distinguished based on the dependence of electron kinetic energy on photon energy.[5] When an unoccupied state, such as LUMO, is probed in a 2PPE process (Figure 1), the absorption of the first photon excites an electron from occupied orbitals to an unoccupied intermediate state; the absorption of a second photon excites this transient electron above the vacuum level. In this case, the change in electron kinetic energy scales with that in photon energy, i.e., $\Delta E_{kin} = 1 \cdot \Delta h\nu$. On the other hand, for two-photon nonresonant excitation from an occupied state, e.g., HOMO, the kinetic energy of the electron ejected scales with two-photon energy, i.e., $\Delta E_{kin} = 2 \cdot \Delta h\nu$. 2PPE can also probe an unoccupied state above the vacuum level, and E_{kin} is independent of photon energy. This can be viewed as a resonant scattering event in which the photoexcited electron resides transiently in the molecular resonance, followed by detachment and detection. Note that this rule-of-thumb of integral slopes need not strictly hold in the presence of strong perpendicular dispersion, as in the case of a bulk Cu band-to-band transition observed previously on

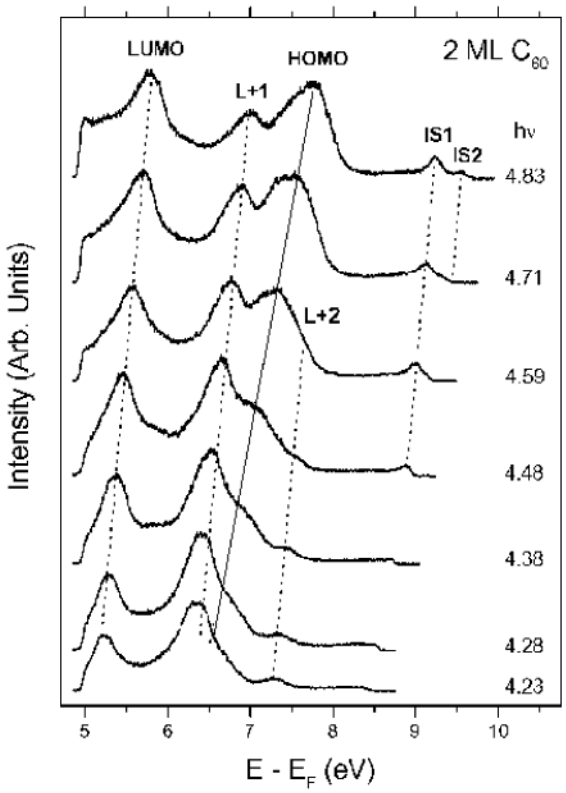

Figure 5. 2PPE spectra of 2 ML C_{60}/Cu(111) taken at the indicated photon energies ($h\nu = 4.23-4.83$ eV). The solid line corresponds to a two-photon dependence of peak position, while the dashed lines indicate one-photon dependences.

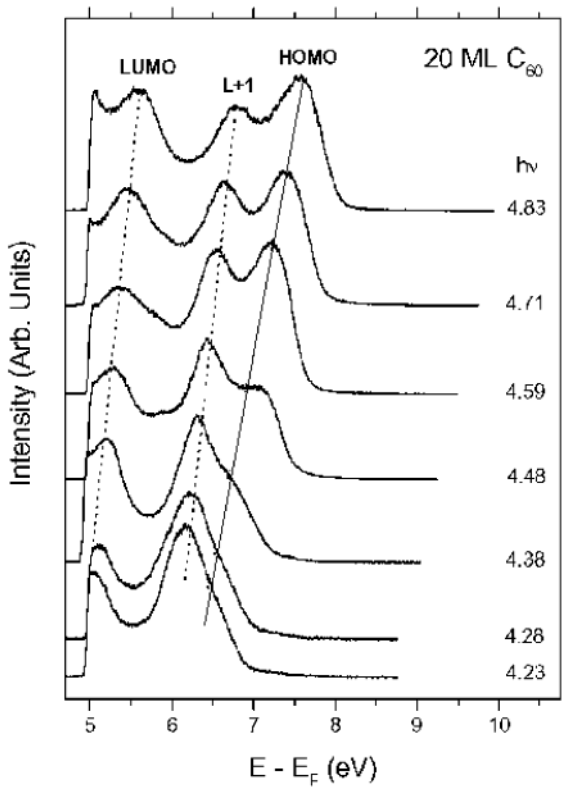

Figure 6. 2PPE spectra of 20 ML C_{60}/Cu(111) taken at the indicated photon energies ($h\nu = 4.23-4.83$ eV). The solid line corresponds to a two-photon dependence of peak position, while the dashed lines indicate one-photon dependences.

Cu(111),[25] but in the present system of narrow-band C_{60}, such deviation is unlikely.

3.3. Multilayer C_{60} Thin Films. The multilayer spectra ($\theta = 2-20$ ML) in Figure 4 are nearly identical, indicating common origins of these peaks. We now establish the energetics of these transitions based on their dependences on photon energy. Figure 5 shows a set of 2PPE spectra taken at $h\nu = 4.23-4.83$ for 2 ML C_{60}/Cu(111). The vertical offset on each spectrum is proportional to the photon energy (note the same treatment in Figures 6 and 7). Six peaks are observed in the photon energy range explored. The position (E_{kin}) of one peak scales with $2h\nu$ while the others scale with 1 $h\nu$. The former arises from an occupied state below the Fermi level and the others are due to unoccupied states below the vacuum level. The energy of the occupied state is determined by

$$E = E_{kin} + \Phi - 2h\nu \quad (1)$$

to be -1.91 eV with respect to E_F at 2 ML. This state is observed at all coverages (see Figure 5 and 6) and is readily identified as the h_u highest-occupied molecular orbital (HOMO) by comparison with PES results.[6,7,11-20] For example, PES revealed the HOMO at -1.7 eV for monolayer C_{60} on Cu(111)[13] and -2.25 eV for thick films.[15]

The energetic positions of unoccupied states are obtained from

$$E = E_{kin} + \Phi - h\nu \quad (2)$$

The two unoccupied states near the vacuum level (high E_{kin} side of the spectra) are image states and will be discussed later. The three unoccupied states (on the low kinetic energy side of the spectra) are at 0.95, 2.16, and 3.05 eV above E_F, and are assigned to the t_{1u} LUMO, t_{1g} LUMO + 1, and h_g,t_{1u} LUMO + 2, respectively. The spacings between these states are consistent with previous results from IPES measurements and theoretical predictions.[6-9] For example, for a thick C_{60} film on Cu(111), IPES puts LUMO, LUMO + 1, and LUMO + 2 at 1.4, 2.6, and 3.6 eV, respectively, above the Fermi level.[13] Note that the LUMO + x levels determined by 2PPE are lower in energy as compared to those from IPES. This issue will be discussed later.

When the C_{60} coverage is increased above 2 ML, the weak spectral features due to image states and the LUMO + 2 level are further attenuated and become invisible at $\theta > 3$ ML. The intense features due to LUMO, LUMO + 1, and HOMO remain nearly unchanged throughout the coverage region investigated. Figure 6 shows a set of 2PPE spectra for 20 ML C_{60}/Cu(111). The three peaks (one occupied and two unoccupied) are assigned as the HOMO (-2.04 eV), the LUMO (0.83 eV), and the LUMO + 1 (2.03 eV). Note a slight downward shift in all states as the coverage increases.

We have also recorded 2PPE spectra for C_{60} thin films as a function of detection angle (from surface normal) and found no evidence of detectable dispersion. The lack of significant band dispersion is in agreement with previous measurements by UPS and IPES.[6,7,11-20]

3.4. Monolayer C_{60}. The identification of C_{60}-derived bands in the 1 ML spectra is less straightforward than for thicker films, considering the lack of sharp features (see Figure 4). Monolayers of C_{60} on single crystal and polycrystalline noble metal surfaces have been studied by a variety of techniques, and the results have been interpreted in terms of charge transfer from the metal to the monolayer, with the extent of electron transfer following Au < Ag < Cu.[11-20] A value of 1.5−2 electron transfer has been estimated for C_{60} monolayers on Cu(111).[11-20]

Figure 7 shows a set of 2PPE spectra for monolayer C_{60} on Cu(111) taken at the indicated photon energies. The two unoccupied states at high kinetic energies are image states

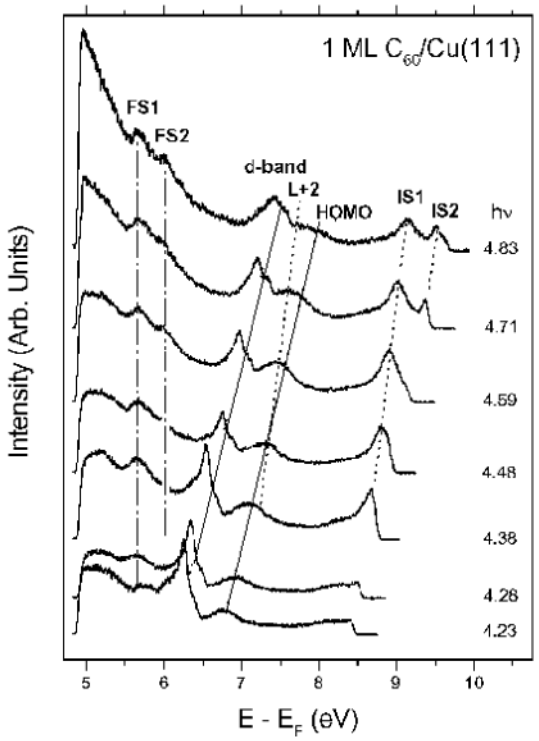

Figure 7. 2PPE spectra of 1 ML C_{60}/Cu(111) taken at the indicated photon energies ($h\nu = 4.23-4.83$ eV). The solid lines correspond to a two-photon dependence of peak position; the dashed lines correspond to one-photon dependence; the dot-dashed lines correspond to zero-photon energy dependence. FS: final state; IS: image state; L: LUMO.

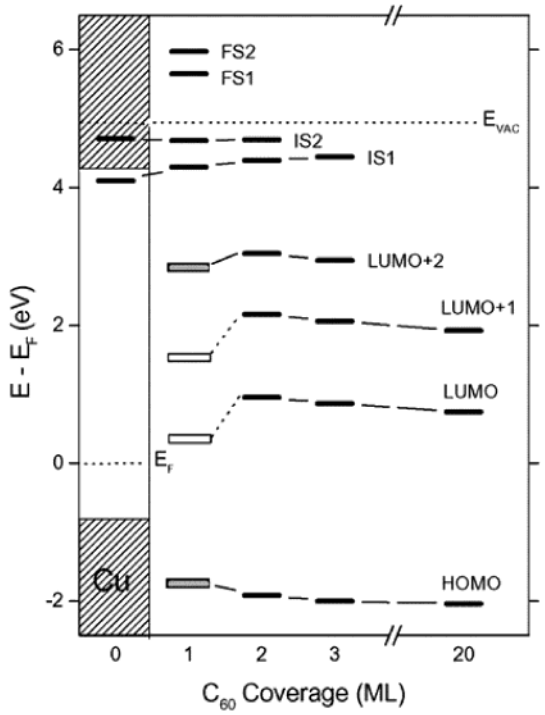

Figure 8. Energy level of molecular orbitals for C_{60}/Cu(111) as a function of adsorbate coverage. The projected band gap in the (111) direction in bulk Cu, the Fermi level, and the vacuum level are also shown.

($n = 1, 2$). At kinetic energies just above the copper d-band, a peak is seen which shifts as an occupied state at low photon energies and as an unoccupied state at higher photon energies. We believe this broad peak corresponds to overlapping features arising from an occupied state at −1.70 eV, the C_{60} h_u HOMO,[13] and an unoccupied state located at 2.85 eV above E_F. Electron transfer to the monolayer requires partial filling of the 3-fold degenerate LUMO. PES−IPES studies of C_{60} films doped with increasing amounts of potassium showed a continuous shift of unoccupied levels downward toward E_F and a gradual filling of the LUMO band.[25] At a potassium dose corresponding to the transfer of 2.7 electrons, the LUMO + 2 was observed at ∼2.7 eV while the lower unoccupied bands were broad and poorly resolved. An IPES spectrum of 1 ML C_{60}/Cu(111) appeared remarkably similar, but explicit assignment of bands was not suggested.[12] Based on these evidences, we assign the unoccupied state at ∼2.85 eV in our 2PPE spectra to the LUMO + 2. For the alkali fullerides, the LUMO filling does not result in strictly rigid band shifts, with the LUMO + 1 to LUMO + 2 separation increasing to 1.3 eV at a filling of ∼3 electrons.[25] Therefore, although they are not resolved, we may estimate the positions of the LUMO + 1 and LUMO at ∼1.55 and 0.35 eV, respectively. This places the LUMO near E_F, as required for electron transfer from the substrate, and supports our assignment of the LUMO + 2. Note that at kinetic energy below that for the d-band, there are two weak features with constant peak positions at different photon energies. The lack of dependence of kinetic energy on photon energy indicates that they are final states (labeled F1 and F2) above the vacuum level, although the exact origins of these peaks are not known.

4. Discussions

Figure 8 summarizes the energetics of all states observed in the present study. The thick solid lines are quantitative determinations from 2PPE, while the gray boxes for 1 ML are approximate positions from the overlapping feature in the spectra. The two open boxes are estimated positions for LUMO and LUMO + 1 at 1 ML coverage. In the following, we discuss three lessons we can learn from these quantitative results: excitation mechanisms, excited-state stabilization, and image potentials.

4.1. Excitation Mechanisms: Intramolecular and Metal-to-Molecule. An occupied state, such as HOMO, is probed in a 2PPE process by coherent two-photon excitation, leaving behind an $N - 1$ final state. This is similar to one-photon photoemission, and the HOMO level determined by 2PPE is identical to that determined by PES. On the other hand, unoccupied states in a molecular film on a metal surface are probed in a 2PPE processes by different possible mechanisms. Two prominent mechanisms for the transient population of unoccupied molecular orbitals are intramolecular excitation and photoinduced metal-to-molecule electron transfer. The insensitivity on film thickness (2−20 ML) of the LUMO and LUMO + 1 features in 2PPE spectra points to the dominance of intramolecular excitation mechanism. The strongly correlated nature of solid C_{60} precludes a molecular band-to-band type of excitation. The intramolecular excitation mechanism is also supported by energetics, namely the presence of 1/2 of the Hubbard U in the band gap determined by 2PPE (see below). The initial state involved in such an intramolecular excitation mechanism may be one of the broad HOMO − n ($n = 0, 1, 2...$) levels.

While the LUMO and LUMO + 1 levels are transiently populated by intramolecular excitation, this may not be the case for the LUMO + 2 level. The LUMO + 2 level is located at ∼3 eV above the Fermi level, or ∼5 eV above HOMO. Thus, the observation of the LUMO at a photon energy as low as 4.23 eV (see Figure 5) is unlikely a result of direct photoexcitation. We believe the LUMO + 2 level is transiently populated by photoinduced electron transfer (ET) from the

metallic substrate to the molecular layer. This interpretation is consistent with the observation that the intensity of the LUMO + 2 feature decreases with increasing film thickness and is not observable at $\theta > 3$ ML. With increasing thickness, the electronic coupling between the C_{60} molecule and the metal surface is expected to decrease. As a result, the transition dipole moment for metal-to-molecule ET excitation should also decrease with coverage.

The observation of this metal-to-molecule ET excitation channel for LUMO + 2 suggests that a similar mechanism likely operates for the transient population of LUMO or LUMO + 1. This ET channel for LUMO or LUMO + 1 may be obscured by the dominant signal from intramolecular excitation. One way to isolate the ET mechanism is to use a pump−probe scheme in which the photon energy of the pump laser pulse is below the energetic threshold for direct photoexcitation. As shown in Figure 8, the LUMO and LUMO + 1 levels may both be populated by excitation photon energies as low as 2 eV. The transiently populated LUMO may be ionized by a probe laser pulse with higher photon energy. This kind of two-color, pump−probe experiments are underway.

4.2. The HOMO−LUMO Gap and 1/2 the Hubbard U. While the position of the HOMO determined by 2PPE agrees with that from previous UPS measurements, the LUMO (or LUMO + 1) level is 0.75 eV lower than that determined by IPES.[6,7,13] As a result, the HOMO−LUMO gap (peak-to-peak separation) from 2PPE is 2.79 eV as compared to the transport gap of 3.5 eV obtained from combined PES−IPES.[6,7] The stabilization of LUMO level is half of the Hubbard U and can be readily attributed to the on-molecule charge correlation energy in the transient excited state. This result confirms our initial prediction, as illustrated in Figure 1. We believe such a stabilization mechanism in 2PPE is generally applicable to most molecular solids with Hubbard U exceeding bandwidth. Only for molecular solids with the largest bandwidth and at very low temperatures can a true band-to-band type of optical excitation be possible.

The coverage-dependent data in Figure 8 show that all the molecular orbital levels decrease with increasing coverage. The maximum stabilization of each energy level is 0.15 eV when C_{60} coverage is increased from 2 to 20 ML. We attribute this additional stabilization to polarization of the surrounding molecular environment for an excited molecule.

4.3. Image Potential States on the Surface of C_{60}. The high kinetic energy features of the 1, 2, and 3 ML spectra arise from unoccupied states within 0.6 eV of the vacuum level. They display dramatically different behavior than the C_{60}-derived molecular orbitals already identified. Unlike the LUMO + n states that exhibit little dispersion, these peaks show nearly free-electron-like parabolic dispersion parallel to the surface with the periodicity of the overlayer lattice (data not shown). Additionally, they are observed only for deposition conditions that produce the greatest degree of order in the superstructure (as determined by LEED). Furthermore, the peak widths are considerably narrower (~0.2 eV fwhm) than the vibrationally broadened C_{60} molecular features (typically ~0.6 eV fwhm). This evidence suggests an origin other than the narrow-band adsorbate levels. We attribute these features to the image states of the C_{60}/Cu(111) system. In a previous IPES study of a C_{60} monolayer on Cu(111), the poorly resolved $n = 1$ image state was reported at a binding energy of 0.8 eV below vacuum, indistinguishable from that of the clean surface.[12] This state was observed only on annealed monolayer films, and there was no evidence of image states at higher coverages deposited at room temperature. Our modified dosing conditions and much improved energy resolution allow us to report accurate binding energies for both the $n = 1$ and $n = 2$ image states for monolayer and multilayer coverages. We find that the $n = 1$ state on 1 ML C_{60}/Cu(111) lies at 0.59 eV below vacuum. It is not clear why the prior study gave a significantly different binding energy, but the coincidence of the reported 1 ML $n = 1$ binding energy with that of the clean surface suggests that patches of clean Cu(111) may have contributed to the signal in this earlier study. This highlights the importance of a highly ordered monolayer prepared by dosing at elevated substrate temperatures. The binding energies of both image states (Figure 8) are seen to decrease with increasing C_{60} coverage. This coverage dependence may indicate that the image states are located within the gap of molecular states/bands.[4,5] It should be noted that image states are only observed on thin films ($\leq$ ~3 ML) for which favorable matrix elements exist for excitation of delocalized metal initial states to the 2D delocalized image states predominantly located near the vacuum interface. Additionally, the likelihood of increased surface roughness at higher coverages may also contribute to the attenuation of image state intensity. A detailed account of image state energetics and dynamics on C_{60} films will appear in a future publication.

Acknowledgment. This work was supported by the National Science Foundation, grant DMR 9982109. G.D. thanks the University of Minnesota Graduate School for a dissertation fellowship.

References and Notes

(1) (a) Schön, J. H.; Kloc, C.; Batlogg, B. *Nature* **2000**, *406*, 702. (b) Schön, J. H.; Kloc, C.; Haddon, R. C.; Batlogg, B. *Science* **2000**, *288*, 656. (c) Schön, J. H.; Kloc, C.; Batlogg, B. *Science* **2001**, *293*, 2432. (d) Schön, J. H.; Kloc, C.; Batlogg, B. *Phys. Rev. Lett.* **2001**, *86*, 3843.

(2) Fauster, T.; Steinmann, W. In *Photonic Probes of Surfaces*; Halevi, P., Ed.; Elsevier: Amsterdam, 1995.

(3) Petek, H.; Ogawa, S. *Prog. Surf. Sci.* **1997**, *56*, 239.

(4) Harris, C. B.; Ge, N. E.; Lingle, R. L.; McNeill, J. D.; Wong, C. M. *Annu. Rev. Phys. Chem.* **1997**, *48*, 711.

(5) Zhu, X.-Y. *Annu. Rev. Phys. Chem.* **2002**, *53*, 221.

(6) Weaver, J. H. *J. Phys. Chem. Solids* **1992**, *53*, 1433.

(7) Rudolf, P.; Golden, M. S.; Bruhwiler, P. A. *J. Electron Spectrosc. Relat. Phenom.* **1999**, *100*, 409.

(8) Laouini, N.; Andersen, O. K.; Gunnarsson, O. *Phys. Rev. B* **1995**, *51*, 17446.

(9) Bohm, B. C.; Schulte, J. *Mol. Phys.* **1996**, *87*, 735.

(10) Lof, R. W.; van Veenendaal, M. A.; Koopmans, B.; Jonkman, B.; Sawatzky, G. A. *Phys. Rev. Lett.* **1992**, *68*, 3924.

(11) Rowe, J. E.; Rudolf, P.; Tjeng, L H.; Malic, R. A.; Meigs, G.; Chen, C. T.; Chen., J.; Plummer, E. W. *Int. J. Mod. Phys.* **1992**, *6*, 3909.

(12) Tsuei, K.-D.; Johnson, P. D. *Solid State Commun.* **1997**, *101*, 337.

(13) Tsuei, K.-D.; Yuh, J.-Y.; Tzeng, C.-T.; Chu, R.-Y.; Chung, S.-C.; Tsang, K.-L. *Phys. Rev. B* **1997**, *56*, 15412.

(14) Hoogenboom, B. W.; Hesper, R.; Tjeng, L. H.; Sawatzky, G. A. *Phys. Rev. B* **1998**, *57*, 11939.

(15) Ohno, T. R.; Chen, Y.; Harvey, S. E.; Kroll, G. H.; Weaver, J. H.; Haufler, R. E.; Smalley, R. E. *Phys. Rev. B* **1991**, *44*, 13747.

(16) Maxwell, A. J.; Bruhwiler, P. A.; Nilsson, A.; Martensson, N.; Rudolf, P. *Phys. Rev. B* **1994**, *49*, 10717.

(17) Tjeng, L. H.; Hesper, R.; Heessels, A. C. L.; Heeres, A.; Jonkman, H. T.; Sawatzky, G. A. *Solid State Commun.* **1997**, *103*, 31.

(18) Hesper, R.; Tjeng, L. H.; Sawatzky, G. A. *Europhys. Lett.* **1997**, *40*, 177.

(19) Tzeng, C.-T.; Lo, W.-S.; Yuh, J.-Y.; Chu, R.-Y.; Tsuei, K.-D. *Phys. Rev. B* **2000**, *61*, 2263.

(20) Cepek, C.; Vobornik, I.; Goldoni, A.; Magnano, E.; Selvaggi, G.; Kroger, J.; Panaccione, G.; Rossi, G.; Sancrotti, M. *Phys. Rev. Lett.* **2001**, *86*, 3100.

(21) Quast, T.; Bellmann, R.; Winter, B.; Gatzke, J.; Hertel, I. V. *J. Appl. Phys.* **1998**, *83*, 1642.

(22) Long, J. P.; Chase, S. J.; Kabler, M. N. *Phys. Rev. B* **2001**, *64*, 205415.

(23) Jacquemin, R.; Kraus, S.; Eberhardt, W. *Solid State Commun.* **1998**, *105*, 449.
(24) Velic, D.; Knoesel, E.; Wolf, M. *Surf. Sci.* **1999**, *424*, 1.
(25) Benning, P. J.; Poirier, D. M.; Ohno, T. R.; Chen, Y.; Jost, M. B.; Stepniak, F.; Kroll, G. H.; Weaver, J. H.; Fure, J.; Smalley, R. E. *Phys. Rev. B* **1992**, *45*, 6899.